

Research Article

In Vitro Antitumor Activity of a Keggin Vanadium-Substituted Polyoxomolybdate and Its ctDNA Binding Properties

Wen Qi,¹ Ying Qin,² Yanfei Qi,¹ Li Guo,¹ and Juan Li¹

¹ School of Public Health, Jilin University, Changchun, Jilin 130021, China

² Medical Services Section, General Hospital of the Jilin Oil Field, Songyuan 138000, China

Correspondence should be addressed to Yanfei Qi; qianfei@jlu.edu.cn

Received 1 August 2014; Accepted 26 August 2014

Academic Editor: Taohai Li

Copyright © 2015 Wen Qi et al. This is an open access article distributed under the Creative Commons Attribution License, which permits unrestricted use, distribution, and reproduction in any medium, provided the original work is properly cited.

A Keggin vanadium-substituted polyoxomolybdate, $K_5\text{PMo}_{10}\text{V}_2\text{O}_{40}$ ($\text{PMo}_{10}\text{V}_2$), has been synthesized and its antitumor effect against HeLa cells was investigated. The calf thymus DNA (ctDNA) binding ability of $\text{PMo}_{10}\text{V}_2$ was also evaluated by UV-Vis absorption spectra and fluorescence spectra. The identity and high purity of $\text{PMo}_{10}\text{V}_2$ was confirmed by elemental analysis and IR analysis. And the antitumor activity test of $\text{PMo}_{10}\text{V}_2$ was carried out on HeLa cancer cells line by MTT assay. The results of MTT assay show that $\text{PMo}_{10}\text{V}_2$ significantly reduced the viability of HeLa cells in a dose-dependent manner and exhibited stronger inhibitory activity against HeLa cells at an IC_{50} of 800 $\mu\text{g}/\text{mL}$, which is more effective than the positive control, 5-Fu ($P < 0.05$). The results of the UV-Vis absorption spectra and fluorescence spectra indicated the groove or outside stacking binding between $\text{PMo}_{10}\text{V}_2$ and ctDNA. These results show that the antitumor activity of $\text{PMo}_{10}\text{V}_2$ may be caused by the interactions between DNA and $\text{PMo}_{10}\text{V}_2$.

1. Introduction

The current interest in polyoxometalates (POMs) keeps on increasing worldwide, not only because of their enormous structural variety, but also their potential applications in multitudinal fields such as catalysis, medicine, and functional materials [1, 2]. Especially, the medicinal properties of POMs have been a subject of interest in drug discovery. In the literature, POMs serve as a few kinds of inorganic medicinal candidates that have been documented to exhibit antiviral activities and antitumor activities [3–6]. For instance, the PM-8 polyoxometalate synthesized by Yamase and coworkers and that has been evaluated for *in vivo* and *in vitro* antitumor activities found to induce apoptotic cell death in human pancreatic cancer cells, AsPC-1, and possesses potent antitumor activity against human Co-4 colon, MX-1 breast, and lung cancer [7–10]. In addition, the group also proposed mechanism that a single electron reduction/oxidation cycle of PM-8 in tumor cells could inhibit the ATP generation [11]. On the other hand, these compounds are less expensive than those of organic medicines, attracting great attention on

the medicinal exploration. During the last 20 years, it has been established that the size, shape, and charge density of many polyoxoanions are strongly relative to their biological activities and toxicity [12, 13].

Cancer is difficult to treat and developing efficient anti-tumor medicines remain one of the most important goals of modern medicinal chemistry research [14]. Cancer starts due to prototype causative factors in a group of cells, leading to DNA damage, thus causing genetic mutations or chromosome structure, the number of different changes, which in turn leads to irreversible changes. DNA is very important genetic substance in any organism and a primary intracellular target for antitumor drugs. The interactions between DNA and small molecules can cause damage in cancer cells and lead to cell death [15]. In recent year the interaction of drugs with DNA and investigation of new effective DNA probes have been focused on the study of small molecular interacting with DNA [16]. POMs are seldom researched in the agents that directly interact with DNA, [17–20], which have shown the ability on inhibiting tumor growth by affecting the mitotic index, the synthesis of DNA, the activity of succinyl

hydrogenase, cytochrome oxidase, and acid phosphatase of tumor cells [21].

As a part of our ongoing antitumor drug discovery, a number of POMs have been synthesized and evaluated for their potential antitumor activities [22–25]. Herein, a Keggin vanadium-substituted polyoxomolybdate, $K_5PMo_{10}V_2O_{40}$ ($PMo_{10}V_2$), was prepared. The antitumor activity against HeLa cells of $PMo_{10}V_2$ were investigated *in vitro*. The results indicate that $PMo_{10}V_2$ exhibits strong antitumor activity against the HeLa cells, indicating that it is a potential antitumor candidate. The calf thymus DNA (ctDNA) binding ability of $PMo_{10}V_2$ was also investigated, using UV-Vis absorption spectra and fluorescence quenching.

2. Experiment

2.1. General Procedures. All solvents and chemicals were used as obtained from commercial supplies. The ctDNA and ethidium bromide (EB) were purchased from Sigma Company. The solution of ctDNA was prepared by dissolving ctDNA in phosphate buffer solution at 4°C under intense stirring for more than 24 h to get a homogeneous solution. Solutions of ctDNA in 10 mM phosphate buffer solution (PBS, 10 mM) of pH 7.4 gave a ratio of UV absorbance at 260 nm and 280 nm; A_{260}/A_{280} was 1.82, indicating that the ctDNA was sufficiently free of protein and need no more further purification. The ctDNA concentration per nucleotide was determined by UV absorbance at 260 nm ($\epsilon_{260} = 6600 \text{ L mol}^{-1} \text{ cm}^{-1}$). And HeLa cancer cell lines, DMEM (Hyclone), Fetal bovine serum (sijiqing), penicillin-streptomycin (Sigma), 3-[4,5-dimethylthiazol-2-yl]-2,5-diphenyltetrazolium bromide (MTT) (Sigma), DMSO (Sigma), and phosphate buffer saline (Sigma) were used for determination of POM cytotoxicity. The elemental analysis of $PMo_{10}V_2$ was estimated by a Leaman inductively coupled plasma (ICP) spectrometer. Infrared spectrum was recorded in the range 400–4000 cm^{-1} on a Nicolet Magna 560 FT/IR Spectrophotometer using KBr pellets. UV-Vis spectra of $PMo_{10}V_2$ in different concentrations of ctDNA were recorded on a Shimadzu U-3010 Spectrophotometer with a 1 cm path length cell. The fluorescence spectra were recorded on a shimadzu RF-5301PC spectrofluorophotometer. The optical absorbance was read on a plate reader (BIO-RAD Co., USA) at a wavelength of 570 nm for MTT.

2.2. Synthesis of $K_5PMo_{10}V_2O_{40}$. The vanadium-substituted heteropolymolybdate $K_5PMo_{10}V_2O_{40}$ ($PMo_{10}V_2$) was synthesized according to the literature [26] and identified by IR spectrum and elemental analysis.

2.3. Cytotoxicity and the Antitumor Activity In Vitro Assay. The antitumor activity of the $PMo_{10}V_2$ on the human cancer cells were tested by the MTT method as described in literature [27]. MTT is a dye that can accept a hydrogen atom. The surviving tumor cells can reduce the yellow MTT to a blue formazan, but the dead tumor cells do not possess this capability. Thus the number of survival cells could be calculated by the change of optical density. HeLa cells

line was used for *in vitro* MTT assay. DMEM medium supplemented with 10% fetal bovine serum and 50 $\mu\text{g}/\text{mL}$ penicillin-streptomycin. $K_5PMo_{10}V_2O_{40}$ and 5-fluorouracil (5-Fu) were sterilized by filtration prior to use. Each agent was dissolved in DMEM to generate the appropriate doses for experimentation. Nontreated cells (DMEM alone) were used as negative controls. The HeLa cells were plated on the 96-well cell culture plates at a density of 5×10^3 cells well^{-1} for 24 h at 37°C in a 5% CO_2 incubator. After that the dilutions of $PMo_{10}V_2$ and 5-Fu at different concentrations were added and allowed to incubate for 24 h. After that the MTT solution (0.02 mL, 5 mg/mL in 0.01 M PBS) was added to each well. The cells were incubated for another 4 h at 37°C and then added DMSO 100 μL per well and shaken for 10 min at room temperature. The samples containing $PMo_{10}V_2$ was dissolved in DMEM medium at 800, 400, 200, 100, 50, 25, and 12.5 $\mu\text{g}/\text{mL}$ concentrations. The 5-Fu was used as the positive control group with the concentration of 400 and 200 $\mu\text{g}/\text{mL}$ in DMEM. The inhibition concentration was determined for each experimental group by comparison with MTT results from nontreated (DMEM alone) cells and calculated using the following formula:

$$\text{Inhibitory rate} = \left(1 - \frac{\text{Mean of the samples}}{\text{Mean of control group}} \right) \times 100\%. \quad (1)$$

2.4. ctDNA Binding Experiments

2.4.1. UV-Vis Absorption Spectra. The absorption titration experiments were performed in absence and presence of ctDNA by sequential addition of specified volume of ctDNA stock solution into a 1 cm path length cuvette containing $PMo_{10}V_2$ solution (100 $\mu\text{M}/\text{L}$) on a U-3010 UV-Vis spectrophotometer. After each addition of ctDNA solution, the absorption spectra were recorded from 200 to 700 nm. The intrinsic binding constant of $PMo_{10}V_2$ with ctDNA was calculated by using the following equation:

$$\frac{[\text{ctDNA}]_T}{(\epsilon_a - \epsilon_f)} = \frac{[\text{ctDNA}]_T}{(\epsilon_b - \epsilon_f)} + \frac{1}{K_b(\epsilon_b - \epsilon_f)}, \quad (2)$$

where, ϵ_a , ϵ_f , and ϵ_b correspond to $A_{\text{obs}}/[\text{PMo}_{10}V_2]$ and the extinction coefficient of free and fully bound $PMo_{10}V_2$, respectively [19]. A plot of $[\text{ctDNA}]_T/(\epsilon_a - \epsilon_f)$ versus $[\text{ctDNA}]_T$, where $[\text{ctDNA}]_T$ is the total concentration of ctDNA in the base pairs unit, gives K_b as the ratio of the slope to intercept [18, 28].

2.4.2. Fluorescence Spectra. The interaction pattern of the $PMo_{10}V_2$ with ctDNA was determined by fluorescence titration method. Fluorescence measurements were carried out by keeping the concentration of $PMo_{10}V_2$ constant and varied concentrations of ctDNA. The fluorescence quenching experiment was performed with EB and the experimental data were plotted according to the Stern-Volmer equation (3):

$$\frac{I_0}{I} = 1 + K_{\text{SV}} [Q]. \quad (3)$$

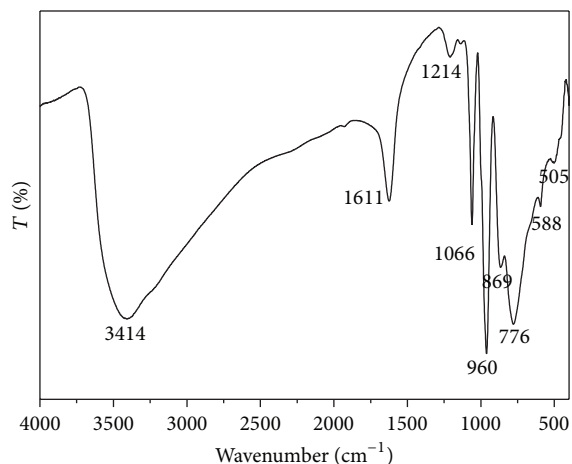


FIGURE 1: IR spectrum of the $\text{PMo}_{10}\text{V}_2$.

(I_0 and I are the fluorescence intensities in the absence and presence of the $\text{PMo}_{10}\text{V}_2$, respectively, $[Q]$ is the concentration of $\text{PMo}_{10}\text{V}_2$ to ctDNA, and K_{SV} is the Stern-Volmer quenching constant which is dependent on the ratio of the bound concentration of EB to the concentration of ctDNA.) Excitation and emission slit widths were set as 5 and 10 nm, respectively. In competition binding experiments, the concentrations of EB and ctDNA were 100 μM and 450 μM , respectively, while $\text{PMo}_{10}\text{V}_2$ concentration varied from 0 to 80 μM . The 522 nm was chosen as the excitation wavelength and the emission spectra were recorded from 200 to 700 nm. The binding mode of $\text{PMo}_{10}\text{V}_2$ with ctDNA was obtained on the basis of previous published methods [19].

2.5. Statistical Analysis. Data were expressed as mean \pm SD. All experiments were performed in triplicate, unless otherwise indicated. Statistical significance was evaluated by one way analysis of variance (ANOVA) combined with Duncan's multiple range tests. The IC_{50} values represent means of quadruplicate determination \pm SD. MTT analysis of multiple comparisons were statistically analyzed using SPSS17 software (significance was established at $P < 0.05$).

3. Results and Discussion

3.1. Determination of $K_5\text{PMo}_{10}\text{V}_2\text{O}_{40}$. The elementary analysis result of $K_5\text{PMo}_{10}\text{V}_2\text{O}_{40}$ is P, 1.47; Mo, 50.62; V 5.10(%) conforms to the calculated result: P, 1.59; Mo, 50.30; 5.23 V(%). The results of the IR spectra analysis to the compound $\text{PMo}_{10}\text{V}_2$ within the range from 400 cm^{-1} to 4000 cm^{-1} using KBr pellets are shown in Figure 1. As shown in Figure 1, the IR spectrum of $\text{PMo}_{10}\text{V}_2$ showed the characteristic asymmetric stretching vibrational peaks at 776, 588, 505 ($\text{Mo}-\text{O}_c-\text{Mo}$), 869 ($\text{Mo}-\text{O}_b-\text{Mo}$), 960 ($\text{Mo}-\text{O}_d$), 1066 and 1214 cm^{-1} (splitting of the triply degenerate PO_4). These peaks suggest that the $\text{PMo}_{10}\text{V}_2$ are successfully synthesized.

TABLE 1: The inhibitory effect of $\text{PMo}_{10}\text{V}_2$.

	Dose/ $\mu\text{g mL}^{-1}$	Hela	
		Inhibitory effect (%)	$\text{IC}_{50}/\mu\text{g mL}^{-1}$
Control	0	0	—
$\text{PMo}_{10}\text{V}_2$	800	53.29	800
	400	29.99	
	200	25.34	
	100	12.9	
	50	7.5	
	25	5.9	
	12.5	5.1	
5-Fu	400	36.02	—
	200	19.49	

3.2. Cytotoxicity and the Antitumor Activity In Vitro Assays. In order to evaluate the antitumor activity of $\text{PMo}_{10}\text{V}_2$, the MTT method was used to detect the activity for HeLa cancer cell lines *in vitro*. A wide range of concentrations (12.5–800 $\mu\text{g/mL}$) of $\text{PMo}_{10}\text{V}_2$ and 5-Fu (200, 400 $\mu\text{g/mL}$) were tested for its toxicity on the HeLa cancer cell line where a dose-dependent cytotoxicity of $\text{PMo}_{10}\text{V}_2$ was observed. The DMEM without drugs was used as control group. It shows that higher concentration of $\text{PMo}_{10}\text{V}_2$ possesses high toxicity on the HeLa cancer cells; at a lower concentration as 12.5 $\mu\text{g/mL}$ there was no obvious sign of cell death. There is a significant difference between control group and experimental group. The inhibitory effect of $\text{PMo}_{10}\text{V}_2$ and 5-Fu is given in Table 1 and the IC_{50} value of $\text{PMo}_{10}\text{V}_2$ is 800 $\mu\text{g/mL}$, which is more effective than the positive control, 5-Fu ($P < 0.05$). It can be concluded that the $\text{PMo}_{10}\text{V}_2$ possesses the antitumor activity with a dose-dependent decrease in the HeLa cells viability, as shown in Table 1 and Figure 2.

3.3. DNA Binding

3.3.1. Absorption Titration. The interaction of $\text{PMo}_{10}\text{V}_2$ with DNA was analyzed by UV-Vis absorption and fluorescence spectroscopic titration. Absorption titration experiments were carried out to determine the binding mode of $\text{PMo}_{10}\text{V}_2$ with ctDNA by monitoring the absorption spectra of $\text{PMo}_{10}\text{V}_2$ in the absence and presence of ctDNA [29]. Figure 3 shows the absorption spectra of $\text{PMo}_{10}\text{V}_2$ in the presence of different concentrations of ctDNA. In the UV region, the $\text{PMo}_{10}\text{V}_2$ performed an intense absorption band around 254 nm. Upon the addition of increasing concentration of ctDNA to $\text{PMo}_{10}\text{V}_2$ solution, a continuing increase in the absorption peak of $\text{PMo}_{10}\text{V}_2$ without any red or blue shift was observed, shown in the Figure 3. The spectroscopic change suggests that there are interactions between $\text{PMo}_{10}\text{V}_2$ and ctDNA.

The titration absorption data were analyzed to evaluate the intrinsic binding constant K_b , which can be calculated based on (2), which was given by the ratio of slope to the intercept in plots from the equation. As shown in the inset

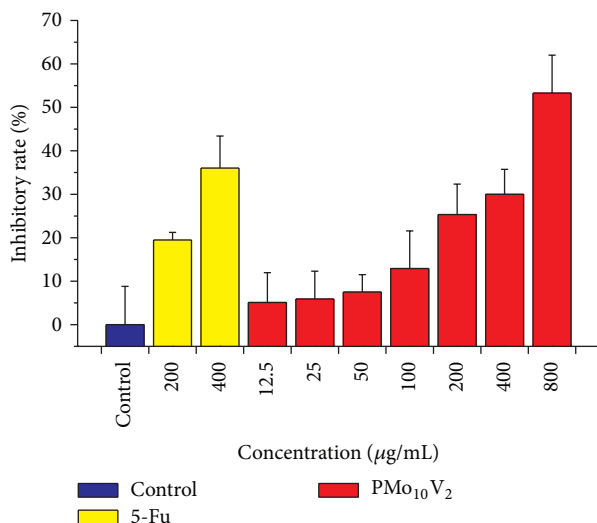


FIGURE 2: The inhibitor effect of control group, 5-Fu groups, and $\text{PMo}_{10}\text{V}_2$ groups on HeLa cells.

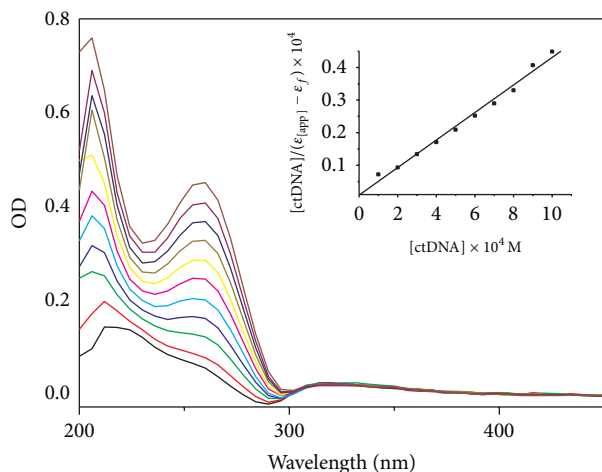


FIGURE 3: Absorption spectra of $\text{PMo}_{10}\text{V}_2$ in PBS at various concentrations of ctDNA. It shows the absorbance changes upon increasing of ctDNA concentrations. Insert: changes of $[\text{ctDNA}]/(\epsilon_{\text{app}} - \epsilon_f)$ versus $[\text{ctDNA}]$ for titration of $\text{PMo}_{10}\text{V}_2$.

of Figure 2, the value of K_b highly depends on the value of R , where $R = [\text{PMo}_{10}\text{V}_2]/[\text{ctDNA}]$. The K_b value ($8.33 \times 10^{-3} \text{ M}^{-1}$) is much smaller than those reported characteristics of classical intercalators ($4 \times 10^4 \text{ M}^{-1}$) [30]. The phenomenon is indicating a weaker binding of ctDNA with $\text{PMo}_{10}\text{V}_2$ than with the classical intercalation interaction. According to the above results, the groove or outside stacking coordinate covalent binding is more probable than intercalative binding between $\text{PMo}_{10}\text{V}_2$ and ctDNA.

3.3.2. Fluorescence Spectroscopic Experiments. To further explore the $\text{PMo}_{10}\text{V}_2$ interaction with ctDNA, a competition experiment with EB, known as the typical intercalator with ctDNA, was investigated. Fluorescent probe technology is a high sensitivity, selectivity detection methods. EB and NR are

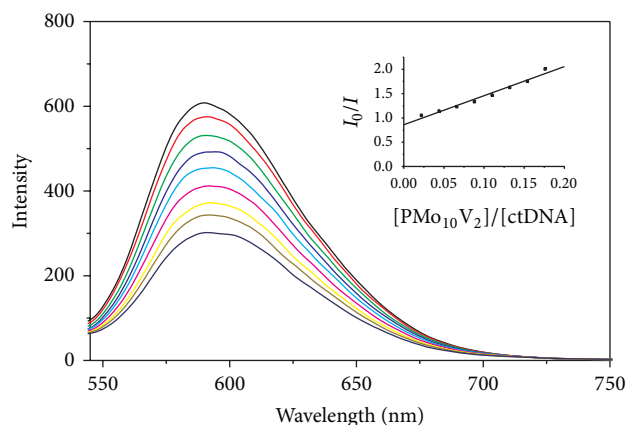


FIGURE 4: The fluorescence spectra of mixed EB ($100 \mu\text{M}$) and ctDNA ($220 \mu\text{M}$) in the presence of different concentrations of $\text{PMo}_{10}\text{V}_2$ in PBS. It shows the fluorescence intensity changes upon increasing concentrations of $\text{PMo}_{10}\text{V}_2$ ($[\text{PMo}_{10}\text{V}_2] = 0, 10, 20, 30, 40, 50, 60, 70, 80 \mu\text{M}$). Insert: Stern-Volmer plot of the fluorescence titration data of EB-ctDNA with different concentration of $\text{PMo}_{10}\text{V}_2$ in PBS.

common used fluorescent probes. EB is a typical indicator of intercalation since it can form soluble complexes with nucleic acids emitting intense fluorescence in the presence of ctDNA due to its strong intercalation between the adjacent ctDNA base pairs. The fluorescence will decrease when the EB dissociate from ctDNA. It was previously reported that the enhanced fluorescence can be quenched by the addition of a second molecule which could replace the bound EB or break the secondary structure of the ctDNA [12, 31]. The Electron transfer or replacement of the molecular fluorophores mechanism has been proposed to account for the quenching effect. For further exploration of ctDNA- $\text{PMo}_{10}\text{V}_2$ interaction, the fluorescence emission of bound EB to ctDNA has been investigated in the presence of $\text{PMo}_{10}\text{V}_2$. The results in Figure 4 show the quenching effect of $\text{PMo}_{10}\text{V}_2$. Upon the addition of increasing concentration of $\text{PMo}_{10}\text{V}_2$, the fluorescence intensity can be quenched. And the reduction of fluorescence intensity depended on the addition of the $\text{PMo}_{10}\text{V}_2$. In the inset of Figure 4, the plots of I_0/I versus $[\text{PMo}_{10}\text{V}_2]$ was a straight line. According to the Stern-Volmer equation, the value of quenching constants was $4.89 \times 10^3 \text{ M}^{-1}$ which is much lower than the corresponding value of EB. $\text{PMo}_{10}\text{V}_2$ does not show any fluorescence whether in ctDNA absence or presence. The maximum binding constant of $\text{PMo}_{10}\text{V}_2$ to ctDNA is much lower than EB, according to the UV-Vis analyses. Hence $\text{PMo}_{10}\text{V}_2$ is not expected to replace the strong bound EB. Therefore, the binding mode of $\text{PMo}_{10}\text{V}_2$ with ctDNA is not intercalation interaction. The result is consistent with the findings obtained from UV-Vis spectral studies.

4. Conclusion

In this study, the synthesis, characterization, antitumor activities, and ctDNA interaction of $\text{PMo}_{10}\text{V}_2$ were investigated.

The results of combined spectroscopic methods reveal that $\text{PMo}_{10}\text{V}_2$ binds to ctDNA by groove or outside stacking binding mode and proved the presence of any direct coordinate covalent bond formation. This binding mode may be explained by considering the high capacity of this $\text{PMo}_{10}\text{V}_2$ for accepting electrons. These results show that $\text{PMo}_{10}\text{V}_2$ as antitumor agents possess high efficacy on Hela cells. The researches of pharmacodynamics, toxicology, and the interaction with DNA on $\text{PMo}_{10}\text{V}_2$ are being further tested.

Conflict of Interests

The authors declare that there is no conflict of interests regarding the publication of this paper.

Authors' Contribution

Wen Qi and Ying Qin contributed equally to this study.


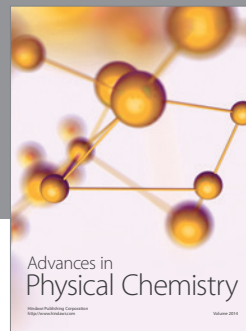
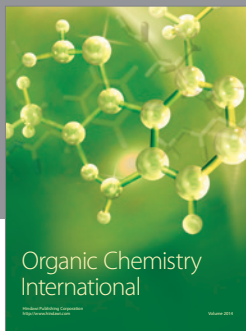
Acknowledgments

This work was financially supported by the National Natural Science Foundation of China (81402719), China Postdoctoral Science Foundation (20100481064 and 2012T50307), Young Scholars Program of Norman Bathune Health Science Center of Jilin University (2013202015), and Jilin Agricultural Product Quality and Safety Project (2011-Y11).

References

- [1] Y. Zhang, J. Q. Shen, L. H. Zheng, Z. M. Zhang, Y. X. Li, and E. B. Wang, "Four polyoxonibate-based inorganic-organic hybrids assembly from bicapped heteropolyoxonibate with effective antitumor activity," *Crystal Growth and Design*, vol. 14, pp. 110–116, 2014.
- [2] L. Grama, A. Man, D.-L. Muntean, S. A. G. Florea, F. Boda, and A. Curticapean, "Antibacterial activity of some saturated polyoxotungstates," *Revista Romana de Medicina de Laborator*, vol. 22, no. 1, 2014.
- [3] L. Wang, K. Yu, B.-B. Zhou et al., "The inhibitory effects of a new cobalt-based polyoxometalate on the growth of human cancer cells," *Dalton Transactions*, vol. 43, no. 16, pp. 6070–6078, 2014.
- [4] Y. L. Zhong, W. Ng, J. X. Yang, and K. P. Loh, "Electrostatically self-assembled polyoxometalates on molecular-dye-functionalized diamond," *Journal of the American Chemical Society*, vol. 131, no. 51, pp. 18293–18298, 2009.
- [5] S. I. Noro, R. Tsunashima, Y. Kamiya et al., "Adsorption and catalytic properties of the inner nanospace of a gigantic ring-shaped polyoxometalate cluster," *Angewandte Chemie—International Edition*, vol. 48, no. 46, pp. 8703–8706, 2009.
- [6] T. Yamase, "Photo- and electrochromism of polyoxometalates and related materials," *Chemical Reviews*, vol. 98, pp. 307–326, 1998.
- [7] T. Yamase and T. Ikawa, "Photochemical study of the alkylammonium molybdates. III. Preparation and properties," *Bulletin of the Chemical Society of Japan*, vol. 50, no. 3, pp. 746–749, 1977.
- [8] H. Fujita, T. Fujita, T. Sakurai, T. Yamase, and Y. Seto, "Antitumor activity of new antitumor substance, polyoxomolybdate, against several human cancers in athymic nude mice," *Tohoku Journal of Experimental Medicine*, vol. 168, no. 2, pp. 421–426, 1992.
- [9] A. Ogata, S. Mitsui, H. Yanagie et al., "A novel anti-tumor agent, polyoxomolybdate induces apoptotic cell death in AsPC-1 human pancreatic cancer cells," *Biomedicine and Pharmacotherapy*, vol. 59, no. 5, pp. 240–244, 2005.
- [10] B. Hasenknopf, "Polyoxometalates: introduction to a class of inorganic compounds and their biomedical applications," *Frontiers in Bioscience*, vol. 10, no. 1, pp. 275–287, 2005.
- [11] C. Streb, C. Ritchie, D. L. Long, P. Kögerler, and L. Cronin, "Modular assembly of a functional polyoxometalate-based open framework constructed from unsupported $\text{AgI} \cdots \text{AgI}$ interactions," *Angewandte Chemie—International Edition*, vol. 46, no. 40, pp. 7579–7582, 2007.
- [12] S. Dianat, A. K. Bordbar, S. Tangestaninejad, B. Yadollahi, S. H. Zarkesh-Esfahani, and P. Habibi, "In vitro antitumor activity of parent and nano-encapsulated mono cobalt-substituted Keggin polyoxotungstate and its ctDNA binding properties," *Chemico-Biological Interactions*, vol. 215, no. 1, pp. 25–32, 2014.
- [13] D.-L. Long, R. Tsunashima, and L. Cronin, "Polyoxometalates: building blocks for functional nanoscale systems," *Angewandte Chemie International Edition*, vol. 49, no. 10, pp. 1736–1758, 2010.
- [14] X. Wang, J. Liu, and M. T. Pope, "New polyoxometalate/starch nanomaterial: synthesis, characterization and antitumoral activity," *Dalton Transactions*, no. 5, pp. 957–960, 2003.
- [15] B. L. Moskovitz, "Clinical trial of tolerance of HPA-23 in patients with acquired immune deficiency syndrome," *Antimicrobial Agents and Chemotherapy*, vol. 32, pp. 1300–1303, 1988.
- [16] D. A. Judd, J. H. Nettles, N. Nevins et al., "Polyoxometalate HIV-1 protease inhibitors. A new mode of protease inhibition," *Journal of the American Chemical Society*, vol. 123, no. 5, pp. 886–897, 2001.
- [17] X. Wang, F. Li, S. Liu, and M. T. Pope, "New liposome-encapsulated-polyoxometalates: synthesis and antitumoral activity," *Journal of Inorganic Biochemistry*, vol. 99, no. 2, pp. 452–457, 2005.
- [18] Y. Ozawa, Y. Hayashi, and K. Isobe, "Structure of triammonium hexahydrogenhexamolybdoxohydroxide(III) hexahydrate," *Acta Crystallographica*, vol. C47, pp. 637–638, 1991.
- [19] T. Mossman, "Rapid colorimetric assay for cellular growth and survival: application to proliferation and cytotoxicity assays," *Journal of Immunological Methods*, vol. 65, no. 1-2, pp. 55–63, 1983.
- [20] P. Jaividhya, R. Dhivya, M. A. Akbarsha, and M. Palaniandavar, "Efficient DNA cleavage mediated by mononuclear mixed ligand copper(II) phenolate complexes: the role of co-ligand planarity on DNA binding and cleavage and anticancer activity," *Journal of Inorganic Biochemistry*, vol. 114, pp. 94–105, 2012.
- [21] F. Arjmand, M. Aziz, and M. Chauhan, "Synthesis, spectroscopic studies of new water-soluble Co(II) and Cu(II) macrocyclic complexes of 4,15-bis(2-hydroxyethyl)-2,4,6,13,15,17-hexaazatricyclodocosane: their interaction studies with calf thymus DNA and guanosine 5' monophosphate," *The Journal of Inclusion Phenomena and Macrocyclic Chemistry*, vol. 61, no. 3-4, pp. 267–278, 2008.
- [22] Z. G. Han, Y. Z. Gao, and C. W. Hu, "Noncovalently connected framework assembled from unusual octamolybdate-based inorganic chain and organic cation," *Crystal Growth and Design*, vol. 8, no. 4, pp. 1261–1264, 2008.
- [23] Y.-Q. Lan, S.-L. Li, X.-L. Wang et al., "Spontaneous resolution of chiral polyoxometalate-based compounds consisting of 3D

- chiral inorganic skeletons assembled from different helical units,” *Chemistry: A European Journal*, vol. 14, no. 32, pp. 9999–10006, 2008.
- [24] H. Yang, S. Guo, J. Tao, J. Lin, and R. Cao, “Hydrothermal syntheses, crystal structures, and magnetic properties of a series of complexes constructed from multinuclear copper clusters and polyoxometalates,” *Crystal Growth and Design*, vol. 9, no. 11, pp. 4735–4744, 2009.
- [25] J. T. Rhule, C. L. Hill, D. A. Judd, and R. F. Schinazi, “Polyoxometalates in medicine,” *Chemical Reviews*, vol. 98, no. 1, pp. 327–358, 1998.
- [26] Y. Tang and J. Zhang, “Direct oxidation of benzene to phenol catalyzed by a vanadium-substituted heteropolymolybdic acid catalyst,” *Journal of the Serbian Chemical Society*, vol. 71, no. 2, pp. 111–114, 2006.
- [27] S. Dianat, A. K. Bordbar, S. Tangestaninejad, B. Yadollahi, S. H. Zarkesh-Esfahani, and P. Habibi, “CtDNA binding affinity and in vitro antitumor activity of three Keggin type polyoxotungstates,” *Journal of Photochemistry and Photobiology B: Biology*, vol. 124, pp. 27–33, 2013.
- [28] S. Mahadevan and M. Palaniandavar, “Spectroscopic and voltammetric studies on copper complexes of 2,9-Dimethyl-1,10-phenanthrolines bound to calf thymus DNA,” *Inorganic Chemistry*, vol. 37, no. 4, pp. 693–700, 1998.
- [29] K. G. Strothkamp and R. E. Strothkamp, “Fluorescence measurements of ethidium binding to DNA,” *Journal of Chemical Education*, vol. 71, no. 1, pp. 77–79, 1994.
- [30] H. Li, X. Y. Lei, D. W. Peng, H. Deng, Z. H. Xu, and Z. H. Lin, “DNA-binding and cleavage studies of novel copper(II) complex with l-phenylalaninate and 1,4,8,9-tetra-aza-triphenylene ligands,” *Journal of Inorganic Biochemistry*, vol. 99, no. 11, pp. 2240–2247, 2005.
- [31] M. N. Dehkordi, A.-K. Bordbar, M. A. Mehrgardi, and V. Mirkhani, “Spectrophotometric study on the binding of two water soluble schiff base complexes of Mn (III) with ct-DNA,” *Journal of Fluorescence*, vol. 21, no. 4, pp. 1649–1658, 2011.



Hindawi

Submit your manuscripts at
<http://www.hindawi.com>

